Organic Electronics 11 (2010) 946–950

Contents lists available at ScienceDirect

Organic Electronics

journal homepage: www.elsevier.com/locate/orgel

Letter

Up-conversion luminescence of crystalline rubrene without any sensitizers

Huihui Liu [a,b], Fei Yan [a,b], Wenlian Li [a,b,*], Chun-Sing Lee [c], Bei Chu [a,b,*], Yiren Chen [a,b], Xiao Li [a,b], Liangliang Han [a,b], Zisheng Su [a,b], Jianzhuo Zhu [a,b], Xianggui Kong [a,b], Ligong Zhang [a,b], Yongshi Luo [a,b]

[a] The Key Laboratory of the Excited State Processes, Chinese Academy of Sciences, 3888-Dong Nan-Hu Road, Changchun 130033, China
[b] Graduate School of the Chinese Academy of Sciences, Beijing 100039, China
[c] Center of Super-Diamond and Advanced Films (COSDAF) and Dept. of Physics & Materials Science, City University of Hong Kong, Hong Kong, China

ARTICLE INFO

Article history:
Received 30 July 2009
Received in revised form 15 January 2010
Accepted 18 January 2010
Available online 25 January 2010

Keywords:
Organic
Up-conversion
Crystallinity

ABSTRACT

Up-conversion luminescence (UCL) in crystalline rubrene samples in absence of any sensitizers under excitation of 980 nm laser was observed. The optimal quasi-single crystal rubrene sample with the highest crystallinity shows the strongest UCL at 610 nm with up-conversion quantum efficiency of 0.19%. The UCL intensity depends on the proportion of orthorhombic crystal phase, particle size, structural defects, and reabsorption of fluorescence in all samples, while amorphous rubrene sample, such as, both polymethylmethacrylate film dispersed with 0.1 wt.% rubrene and 0.5×10^{-3} M rubrene chloroform solution, do not exhibit UCL. According to the dependence of the integral UCL intensity on the excitation power density of 980 nm laser, a two-photon absorption feature in our UCL system was obtained. The mechanism of UCL process was also discussed in detail.

Up-conversion luminescence (UCL) in organic materials has recently become a subject of much research interest for its potential applications in optoelectronic devices [1–4]. Examples include, two-photon absorption (TPA) for various application including up-converted lasing [1], two-photon photodynamic therapy [2], two-photon optical power limiting [3] and two-photon three-dimensional micro-fabrication [4]. Theoretical basis for simultaneous absorption of two photons was developed by Goeppert-Mayer in 1931 [5]. Up-conversion induced luminescence differs from single photon emission based on conventional one-photon absorption. UCL can be achieved through different processes after TPA [6,7]. UCL processes so far reported were mostly observed in solutions [8–10] and in amorphous films [11], typically requiring assistance of one or two sensitizers [11–13]. In sensitized UCL systems, annihilation of two triplet states can lead to a singlet state that can relax to the ground state via radiation. Such triplet–triplet annihilation (TTA) in organic dyes is considered a prominent mechanism for the up-converted delayed fluorescence [14,15]. In this work, we demonstrate red UCL of rubrene crystalline samples under excitation of 980 nm laser. An UCL peaking at 610 nm with an up-conversion quantum efficiency of about 0.19% was obtained. We found that the UCL intensity depends on the proportion of orthorhombic phase, crystal size, structural defects, and reabsorption of fluorescence. It is interesting that unlike other two-photon based emission systems [8,9,16], the present system does not require any sensitizer.

Rubrene samples Ru-1, Ru-2, and Ru-3 were commercially available from XiAn Ruilian Company. According to the manufacturer, the three samples were obtained via different sublimated purification processes. All these three samples were twice sublimed at 10^{-6} torr and collected at slightly different temperatures. To investigate the effects of crystal size, Ru-4 was prepared by slightly grinding Ru-1

* Corresponding authors. Address: The Key Laboratory of the Excited State Processes, Chinese Academy of Sciences, 3888-Dong Nan-Hu Road, Changchun 130033, China.
E-mail addresses: wllioel@yahoo.com.cn (W. Li), beichubox@hotmail.com (B. Chu).

1566-1199/$ - see front matter © 2010 Elsevier B.V. All rights reserved.
doi:10.1016/j.orgel.2010.01.018

with an agate mortar to obtain a corresponding sample with a smaller average grain size. Samples for photoluminescence (PL) measurements were prepared by pressing powder of the materials into aluminum cans to form tablets of 4 mm in diameter and 1 mm in thickness. Special cares have been devoted to make the powder in the tablets as densely packed as possible. Nevertheless, it is expected that due to the different crystal sizes and shapes, the packing densities of samples can be slightly different. Intensities of the UCL spectra so measured are thus not straightly quantitative. Hence, when comparing the absolute PL intensities of different samples, there can be small variations due to different packing densities.

XRD spectra were measured using a Siemens D5005 diffractometer with Cu-Kα radiation (λ = 1.5418 Å). Field emission scanning electron microscopy (FE-SEM) was carried out on a Hitachi S-4800 electron microscope. UCL spectra were measured under excitation of continuous 980 nm semiconductor laser with a maximum power of 2 W at an area of 0.01 cm^2. A Spectrometer with Spex 1403 photomultiplier with a boxcar averager was used to record the spectra. Conventional single photon PL spectra of crystalline samples under continuous 325 nm He–Cd laser were recorded by a UV-Laboratory Raman Infinity (n°9/35 INF, made by Jobin Yvon Company) with a resolution of 2 cm^{-1}. For comparison, PL measurements were also carried out on spin-coated thin film of polymethylmethacrylate (PMMA) doped with 0.1 wt.% rubrene and 0.5×10^{-3} M rubrene chloroform solution. The PL decay curves were measured by a two channel TEKTRONIX TDS-3052 oscilloscope and a Spectrometer with Spex 1403 photomultiplier under excitation of a 980 nm OPO laser and a 355 nm YAG:Nd^{3+} laser. The response time of the measurement system is about 30 ns and the lifetime shorter than 100 ns could not be exactly measured and overestimated with an error about several tens nanoseconds.

Fig. 1 shows X-ray diffraction (XRD) spectra of the four different rubrene powder samples. The main peaks in the XRD spectrum of Ru-1 can be indexed to the (0, 0, 2) and (0, 0, 6) planes of orthorhombic rubrene crystal [17]. Intensities of the (0, 0, 4) and the (0, 0, 8) peaks are much lower than those of (0, 0, 2) and (0, 0, 6). Besides the (0, 0, 2n) peaks, XRD spectra of Ru-2 and Ru-3 also show peaks corresponding to the (2, 0, 0), (2, 2, 0), (3, 1, 1), and (4, 2, 0) planes of a face-centered cubic (FCC) structure. It can also be seen that the (0, 0, 2) peak of the orthorhombic phase in Ru-2 and Ru-3 not only have lower relative intensities, but also be widened. The XRD results suggest that Ru-1 contains pure orthorhombic phase with a highly preferred orientation, while both Ru-2 and Ru-3 consist of orthorhombic and FCC phases. XRD spectrum of Ru-4 is virtually the same as that of Ru-1 which confirms that the grinding did not change the crystal structure. In addition, through comparing the intensities and widths of the diffraction peaks, it is concluded that Ru-1 and Ru-3 have the highest and the lowest crystallinity, respectively.

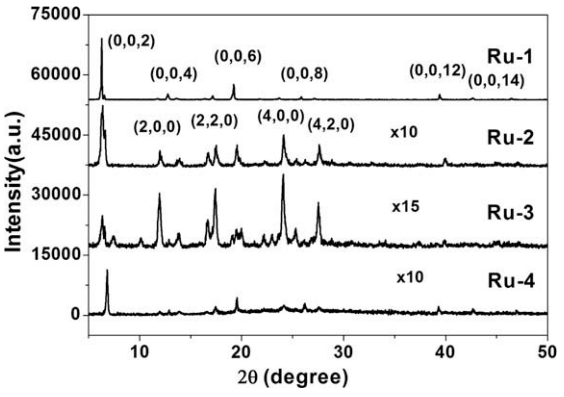

Fig. 1. XRD patterns of crystalline samples Ru-1, Ru-2, Ru-3, and Ru-4.

SEM images of the four crystalline samples are shown in Fig. 2. It can be seen that these samples have distinctly different crystal shapes and crystal sizes, which are about 40 μm, 15–30 μm, 10–20 μm, and 20 μm for Ru-1, Ru-2, Ru-3, and Ru-4, respectively. Crystalline features (sharp angles and edges, etc.) can be clearly observed in all samples. From SEM photographs, we can see that Ru-4 and Ru-1 have similar morphologies. It appears that the grinding of Ru-1 has broken the longer crystals into particles of smaller aspect ratios. On the other hand, Ru-2 and Ru-3 are respectively dominated by plate-like and short-rod crystals.

Fig. 3 shows UCL spectra of the four samples at room-temperature (RT) under the illumination of 980 nm laser. It can be seen that Ru-1 and Ru-3 give the highest and lowest UCL intensities, respectively. As mentioned in the experimental section, possible differences in packing densities of four samples might influence UCL intensities. However, when the conventional PL spectra (Fig. 4) of the four samples (which are exactly the same samples used for the UCL measurements) are compared, it can be seen that Ru-1 has lower PL intensity than Ru-2 and Ru-3. These results suggest that the possible packing density differences should not be a dominating factor on the relative UCL and conventional PL intensities of Ru-1, Ru-2, and Ru-3. On the other hand, as shown in Fig. 1, Ru-1 has a strong (0, 0, 2) texture. Hence, the highly preferred (0, 0, 2) orientation might be a possible cause for the highest UCL intensity. To check this, UCL intensities of Ru-1 were measured again upon tilting the samples to different angles with respect to the incident beam. No obvious change in UCL intensity has been observed. This suggests that the crystal orientation should not influence the UCL intensity.

Fig. 1 shows that Ru-1 consists purely orthorhombic phase, while Ru-2 and Ru-3 are mixtures of orthorhombic and FCC phases. The UCL intensity increases with the ratio of orthorhombic phase to FCC phase. Under the hypothesis that the orthorhombic phase gives the higher UCL intensity than the FCC phase, the UCL intensity order of Ru-1 > Ru-2 > Ru-3 can be consistently explained. Furthermore, Ru-1 has higher UCL (Fig. 3) and conventional PL (Fig. 4) intensities than Ru-4. This suggests that a larger grain size should increase both the UCL and conventional PL. One possible reason for this is stronger scattering effect in the sample with smaller grain size. It should also be pointed out that the UCL peak position of Ru-3 (594 nm) differs obviously from that (610 nm) of the other three samples, and the reasons are not clear.

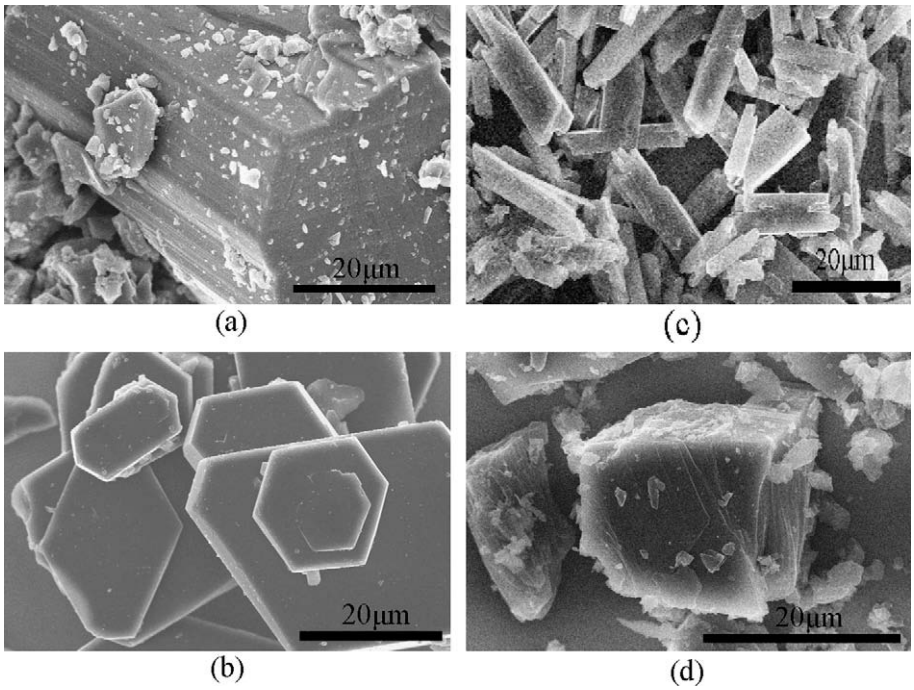

Fig. 2. SEM photographs of Ru-1 (a), Ru-2 (b), Ru-3 (c), and Ru-4 (d) samples.

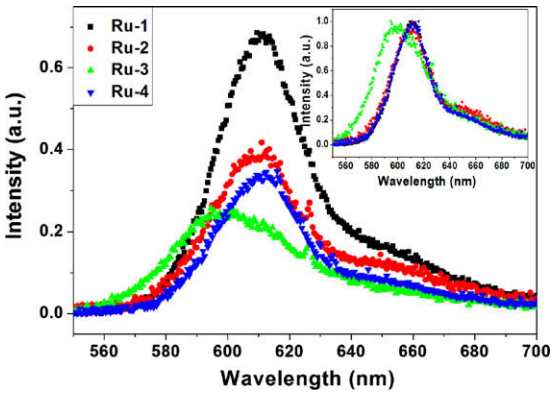

Fig. 3. UCL spectra of Ru-1, Ru-2, Ru-3, and Ru-4 at RT. Inset: Unitary UCL spectra of all samples at RT.

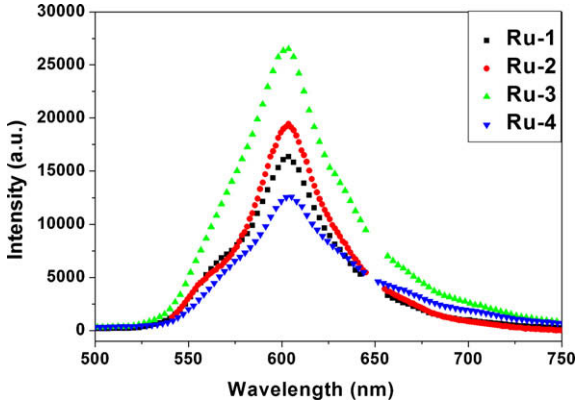

Fig. 4. Single photon emission spectra of samples Ru-1, Ru-2, Ru-3, and Ru-4 (λ_{ex} = 325 nm). Since the intense 650 nm laser line of He–Cd laser overlapped in the spectra, the spectra were drawn after the subtraction of 650 nm line.

Besides the influence of crystal phases and grain size on the difference of UCL intensities at RT, chemical impurities, structural defects, and reabsorption of fluorescence were also taken into account because these factors are related to the luminescence properties of crystal materials [18]. In our work, all samples were sublimed twice at 10^{-6} torr, so that the effect of chemical impurity could be ignored. The samples with lower crystallinity (Ru-2 and Ru-3) and the grinded sample (Ru-4) must have more structural defects than Ru-1. On the other hand, the blue-shift of photo-absorption and the red-shift of the emission peak of rubrene single crystal comparing with Rubrene solution were observed [19], which will lead to the suppression of reabsorption of fluorescence and the increase of fluorescence intensity. Therefore, quasi-single sample Ru-1 shows the highest UCL intensities at RT.

Fig. 5 shows the UCL spectra of the four samples at 77 K. It can be seen that the relative intensities of the samples are similar to those at RT (Fig. 3). One major difference from RT spectra is that the emission bands in all samples shift to shorter wavelength. At low temperature the oscillation of molecular crystal lattice mitigates so that the emission bands shift to higher energy [20].

Fig. 6 shows the dependence of the integral UCL intensity of Ru-1 on the excitation power density at RT and 77 K. At both temperatures, the UCL integral intensities show

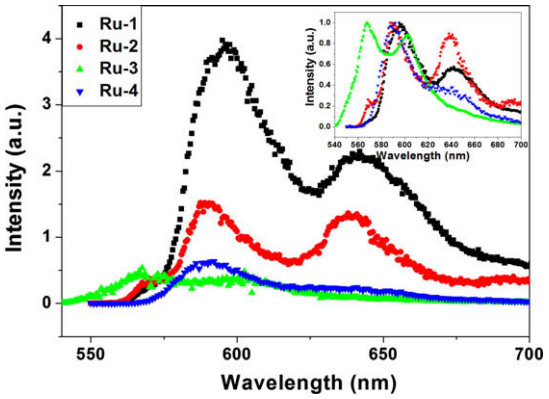

Fig. 5. UCL spectra of Ru-1, Ru-2, Ru-3, and Ru-4 at 77 K. Inset: Unitary UCL spectra of all samples at 77 K.

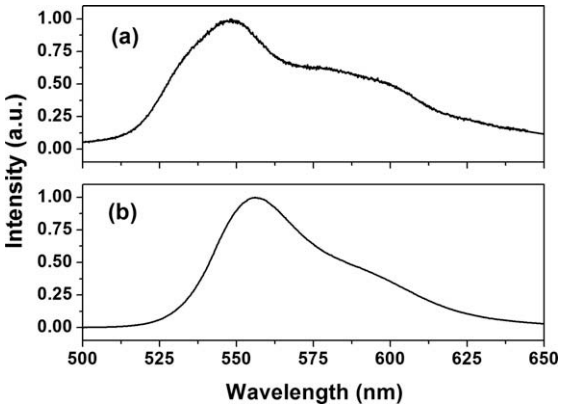

Fig. 7. Single photon emission spectra of 0.1wt.% rubrene dispersed PMMA film by spin-coated from chloroform solution (a) and 0.5×10^{-3} M rubrene chloroform solution (b) (λ_{ex} = 325 nm).

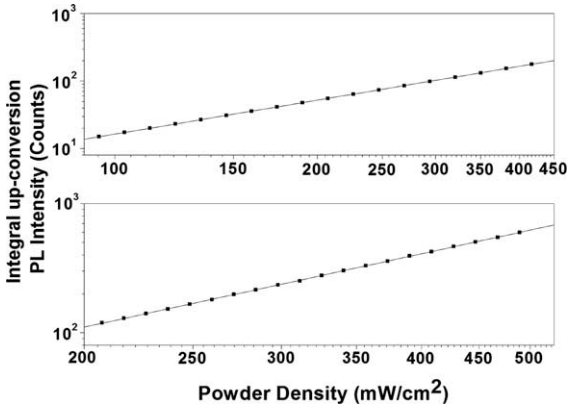

Fig. 6. The dependence of the integral UCL intensity of Ru-1 on the excitation power density of 980 nm laser at RT (a) and 77 K (b).

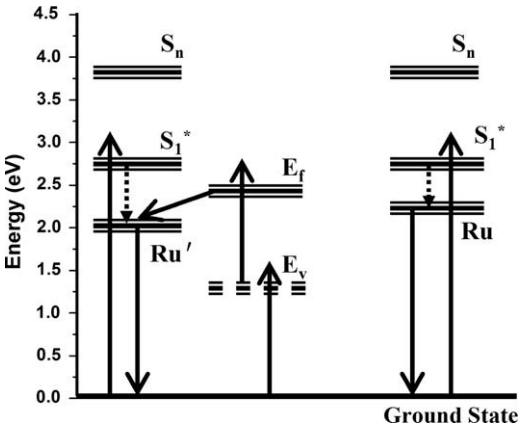

Fig. 8. The schematic level diagram of single- and two-photon emission and the energy transfer processes in UCL. S_1^*: The excited singlet state corresponding to UV laser illumination, E_f: The final state that is the second photon arrives, Ru: The energy level of single photon emission, Ru′: The energy level of UCL.

power law relationships to the excitation power density. The slopes of the fitted straight lines for RT and 77 K are 1.67 and 1.88, respectively, indicating that the UCL of rubrene crystal belongs to TPA process [21].

We also have measured UCL of 0.1 wt.% rubrene dispersed in PMMA film by spin-coated from their chloroform solution and 0.5×10^{-3} M rubrene chloroform solution under excitation of 980 nm laser. However, no UCL was observed; while the film and solution show conventional yellow PL around 550 nm upon illumination of 325 nm laser (Fig. 7). The distance between rubrene molecules in crystalline materials is expected to be much closer so that a stronger intermolecular interactional force produces. It is considered that the interaction between rubrene molecules in crystal is much stronger than that of dispersed rubrene molecules in solid matrix or in solution [19,22]. In other word, there should be no excitonic state corresponding to UCL emission level (610 nm) in rubrene film or solution [19]. Therefore, rubrene dispersed PMMA film or solution samples could not give UCL emission under excitation of 980 nm laser, but isolated rubrene molecules can be excited by 325 nm UV light, as shown in the right of Fig. 8.

In order to deeply investigate the mechanism of UCL process, we measured the decay curves of UCL and conventional PL of crystalline rubrene, and fitted the two lifetimes according to the equation: $y = A_1 * e^{-x/t_1} + A_2 * e^{-x/t_2}$. The results were t_1 = 68 ns (A_1 = 0.80346), t_2 = 472 ns (A_2 = 0.07556) and t_1 = 43 ns (A_1 = 9.99468), t_2 = 506 ns (A_2 = 0.02116) for up-conversion and conventional PLs, respectively. Considering the spectra of up-conversion and conventional PLs, we attribute the shorter lifetime and the longer lifetime to 610 nm emission and 650 nm emission, respectively, because the longer lifetime component presents a little proportion. The 650 nm emission is attributed to the emission of rubrene crystals which exist in small amounts in rubrene samples and this emission is the result of molecular interactions that is similar to the 610 nm emission [22]. Meanwhile, when excited by pulse laser, we can not capture the spectra of up-conversion

and conventional emissions of crystalline rubrene using our spectral measurement system even though we can see the bright light with our eyes, therefore the 610 nm emission should be less than the response time of our system (30 ns). That is, the lifetime of UCL is similar to that of single photon emission. The spectra in Figs. 3–5 were obtained under excitation of continuous 980 nm semiconductor laser and 325 nm He–Cd laser.

Considering that the lifetime of UCL through TTA is far longer than that of single photon emission, we think that the UCL process of crystalline rubrene would be arisen from TPA rather than from TTA. Under excitation of 980 nm infrared laser, as there are no sensitizers in the system, there must be a virtual state with a short lifetime (of the order of a few femto-seconds) playing a very important role in TPA process. As infrared light passes through crystalline rubrene molecules, the virtual state may form and exist for a very short duration [23–25]. If a second photon arrives before this virtual state decayed, TPA can result. The probability of TPA scaling with the square of the light intensity leads to a highly localized photon excitation. Therefore, TPA involves the concerted interaction of both photons that combine their energies, and then produces an electronic excitation similar to that conventionally caused by a single photon of a correspondingly shorter wavelength. Differing from single-photon absorption, the probability is squarely proportional to the incident intensity, as proved by Fig. 5 [23]. In crystalline rubrene, the second photon arriving level, also named as the final level (E_f), lies at 2.51 eV. After absorbed two 980 nm photons, UCL occurs through energy transfer from E_f to UCL level (2.03 eV), as shown in the left of Fig. 8. More detail mechanism for our UCL system is under studying.

UCL of crystalline rubrene samples under excitation of 980 nm infrared laser was demonstrated. It is interesting that it needs no assistance of any sensitizing materials. The UCL intensity increases as the proportion of orthorhombic crystal phase increases. Up-conversion quantum efficiency up to 0.19% was observed at RT in a sample with high phase purity of orthorhombic crystal. A large grain size appeared to have positive influences, while crystal orientation was observed to have little influence on the UCL intensity. UCL was not observed in all non-crystalline rubrene samples. The UCL is attributed to the excitonic state via stronger intermolecular interaction in the crystalline rubrene. It is well-known that most reported organic up-conversion lasers were in solutions which can limit certain applications [26], therefore, this special UCL system could be used to design new up-conversion optical systems.

Acknowledgements

This work was supported by the National Natural Science Foundation of China (Grant No. 10604054 and 60878027), Pillar Project in Burea of Science & Technology of Changchun city (08KZ24), and Knowledge Innovation Project of The Chinese Academy of Sciences (KJCX2-YW-M11).

References

[1] A. Mukherjee, Appl. Phys. Lett. 62 (1993) 3423.
[2] J.D. Bhawalkar, N.D. Kumar, C.F. Zhao, P.N. Prasad, J. Clin. Med. Surg. 37 (1997) 510.
[3] G.S. He, G.C. Xu, P.N. Prasad, B.A. Reinhardt, J.C. Bhatt, A.G. Dillard, Opt. Lett. 20 (1995) 43.
[4] B.H. Cumpston, S.P. Ananthavel, S. Barlow, D.L. Dyer, J.E. Ehrlich, L.L. Erskine, A.A. Heikal, S.M. Kuebler, I.Y.S. Lee, D.M. Maughon, Nature 51 (1999) 398.
[5] M.G. Mayer, Ann. Phys. 9 (1931) 273.
[6] R. Schroeder, W. Graupner, U. Scherf, B. Ullrich, J. Chem. Phys. 116 (2002) 3449.
[7] C. Bauer, B. Schnabel, E.B. Kley, U. Scherf, H. Giessen, R. Mahrt, Adv. Mater. 14 (2002) 673.
[8] R.R. Islangulov, D.V. Kozlov, F.N. Castellano, Chem. Commun. 30 (2005) 3776.
[9] W. Zhao, F.N. Castellano, J. Phys. Chem. A. 110 (2006) 11440.
[10] S. Baluschev, T. Miteva, B. Minch, V. Yakutkin, G. Nelles, A. Yasuda, G. Wegner, J. Appl. Phys. 101 (2007) 023101.
[11] P.E. Keivanidis, S. Baluschev, T. Miteva, G. Nelles, U. Scherf, A. Yasuda, G. Wegner, Adv. Mater. 15 (2003) 2095.
[12] F. Laquai, G. Wegner, C. Im, A. Busing, S. Heun, J. Chem. Phys. 123 (2005) 074902.
[13] S. Baluschev, F. Yu, T. Miteva, S. Ahl, A. Yasuda, G. Nelles, Nano Lett. 12 (2005) 2482.
[14] D. Hertel, H. Bässler, R. Guentner, U. Scherf, J. Chem. Phys. 115 (2001) 10007.
[15] A. Gerhard, H. Bässler, J. Chem. Phys. 117 (2002) 7350.
[16] S. Baluschev, V. Yakutkin, G. Wegner, T. Miteva, G. Nelles, A. Yasuda, S. Chernov, S. Aleshchenkov, A. Cheprakov, Appl. Phys. Lett. 90 (2007) 181103.
[17] E. Menard, A. Marchenko, V. Podzorov, M.E. Gershenson, D. Fichou, J.A. Rogers, Adv. Mater. 18 (2006) 1552.
[18] R. Katoh, K. Suzuki, A. Furube, M. Kotani, K. Tokumaru, J. Phys. Chem. C. 113 (2009) 2961.
[19] A. Saki, S. Seki, T. Takenobu, Y. Iwasa, S. Tagawa, Adv. Mater. 20 (2008) 920.
[20] V.M. Agranovich, G.F. Bassani, J. Knoester, G.C. La Rocca, A.M. Kamchatnov, M. Hoffmann, V.I. Yudson, D.G. Lidzey, in: V.M. Agranovich, D. Taylor (Eds.), Thin Films and Nanostructures: Electronic Excitations in Organic Based Nanostructures, Amsterdam, 2003, pp. 1–96.
[21] Y.Q. Lei, H.W. Song, L. Yang, L. Yu, Z. Liu, J. Chem. Phys. 123 (2005) 174710.
[22] X.H. Zeng, D.Q. Zhang, L. Duan, L.D. Wang, G.F. Dong, Y. Qiu, Appl. Surf. Sci. 253 (2007) 6047.
[23] K.D. Belfield, K.J. Schafer, Y. Liu, X. Ren, E. Stryland, J. Phys. Org. Chem. 13 (2000) 837.
[24] D.I. Lee, T. Goodson III, J. Phys. Chem. B. 110 (2006) 25582.
[25] F. Terenziani, C. Katan, E. Badaeva, M. Blanchard-Desce, Adv. Mater. 20 (2008) 4641.
[26] G.S. He, L. Yuan, P.N. Prasad, A. Abbotto, A. Facchetti, Opt. Commun. 140 (1997) 49.